JOURNAL OF ENZYME INHIBITION AND MEDICINAL CHEMISTRY
2025, VOL. 40, NO. 1, 2467798
https://doi.org/10.1080/14756366.2025.2467798

Taylor & Francis
Taylor & Francis Group

RESEARCH ARTICLE

OPEN ACCESS Check for updates

Discovery of a novel PLK1 inhibitor with high inhibitory potency using a combined virtual screening strategy

Zhen Xu[a#], Lixia Guan[b#], Yuting Wang[b], Miao-Miao Niu[b], Yashi Ruan[a], Cen Xu[a] and Li Yang[a]

[a]Department of Oncology, Urology and Reproductive Medicine, The Affiliated Taizhou People's Hospital of Nanjing Medical University, Taizhou, China; [b]Department of Pharmaceutical Analysis, China Pharmaceutical University, Nanjing, China

ABSTRACT

PLK1 is essential for cell cycle regulation and proliferation, and its elevated expression in prostate cancer is associated with high tumour grade. Therefore, PLK1 inhibition is considered a promising strategy for the treatment of prostate cancer. Here, we identified five compounds (Hits 1-5) targeting the kinase domain (KD) of PLK1 using a combined virtual screening approach. Hits 1-5 all had picomolar (pM) inhibitory potency against PLK1. Notably, Hit-4 showed the strongest inhibitory activity against PLK1 (IC_{50} = 22.61 ± 1.12 pM) and displayed high selectivity for PLK1. Meanwhile, molecular dynamics (MD) simulations revealed that the complex formed by Hit-4 and PLK1 remained stable. Importantly, Hit-4 exhibited potent inhibitory effects on the proliferation of DU-145 prostate cancer cells (IC_{50} = 0.09 ± 0.01 nM). In conclusion, Hit-4 is a potent and highly selective antitumor candidate with therapeutic potential for prostate cancer.

ARTICLE HISTORY
Received 23 December 2024
Revised 5 February 2025
Accepted 10 February 2025

KEYWORDS
Polo-like kinase 1 (PLK1); prostate cancer (PCa); pharmacophore screening; docking screening

Introduction

Prostate cancer (PCa) is the second most commonly diagnosed malignancy and the fifth leading cause of cancer death in men worldwide[1]. Current treatments for prostate cancer include chemotherapy, radiotherapy, surgery, and hormone therapy[2,3]. Although a number of drugs have been tested and approved for use in the early stages of the disease, the heterogeneity of tumours and drug resistance remain a major challenge in the treatment process[2,4]. Androgen deprivation therapy initially shows a period of efficacy, but it is common for the disease to gradually progress to castration-resistant prostate cancer (CRPC)[5,6]. In addition, most of these treatments have limited efficacy in patients with advanced disease and are associated with significant side effects[2,7]. Therefore, the discovery of potential drug candidates with low side effects and high efficacy for prostate cancer therapy is necessary.

Polo-like kinase 1 (PLK1), a serine/threonine kinase, is central to the regulation of the cell cycle and cell proliferation[8,9]. PLK1 is localised to critical mitotic structures and functions as a key regulator of the mitotic process, involved in mitotic entry, centrosome maturation, sister chromatid separation, and the initiation of cytokinesis[10–12]. Given its important role in mitosis, PLK1 is overexpressed in many types of tumours and the elevated expression levels of PLK1 seem to be associated with the aggressiveness and poor prognosis of a wide range of cancers[13–16]. Research shows that the expression levels of PLK1 are significantly elevated in prostate cancer tissue compared to normal prostate cells and correlate with high tumour grade, suggesting that PLK1 is an important factor in the growth and progression of prostate cancer[17–19]. Furthermore, PLK1 is one of the top five signalling pathways upregulated after castration, and downregulation of the PLK1 gene inhibits mitosis in prostate cancer cells[19–21]. Therefore, a therapeutic approach targeting PLK1 may be a promising approach for the treatment of prostate cancer.

DU-145 cells are derived from prostate cancer that has metastasised to the brain and have intermediate metastatic potential[22]. DU-145 cells are androgen insensitive and do not express prostate specific antigen (PSA), which is particularly important for studying the role of PLK1 inhibitors in CRPC[23]. Meanwhile, DU-145 cells showed high levels of PLK1 mRNA and protein expression, and several PLK1 inhibitors significantly inhibited the proliferation of DU-145 cells[24,25]. Therefore, DU-145 cells were used in this study to evaluate the antiproliferative activity.

PLK1 contains a highly conserved catalytic kinase domain (KD) at the N-terminus and a Polo-box domain (PBD) at the C-terminus[26–28]. The KD is responsible for the kinase activity of PLK1 and serves as a key factor in the modulation of cell cycle progression by PLK1, while the PBD modulates the subcellular localisation and function of PLK1 by binding to specific phosphorylated substrates[29–31]. The KD and PBD domains of PLK1 are intrinsic targets for the development of PLK1 inhibitors[32,33]. To date, several PLK1 inhibitors have entered the testing phase of clinical

CONTACT Yashi Ruan ruan.ys@gmail.com; Cen Xu cenxu263128@163.com; Li Yang proyangli@163.com Department of Oncology, Urology and Reproductive Medicine, The Affiliated Taizhou People's Hospital of Nanjing Medical University, Taizhou 225300, China
[#]These authors contributed equally to this work.

Supplemental data for this article can be accessed online at https://doi.org/10.1080/14756366.2025.2467798.

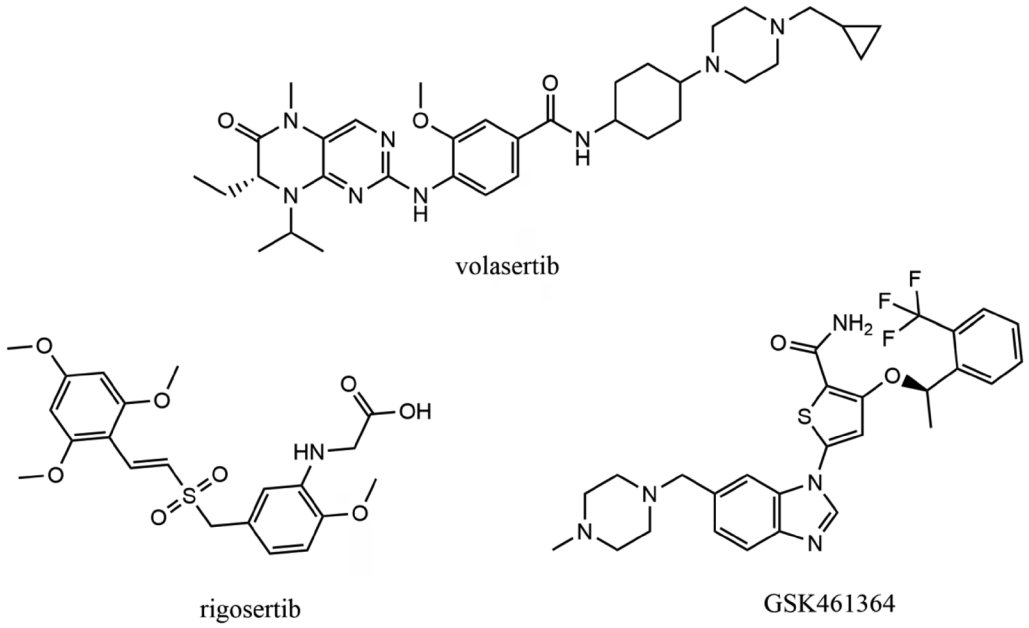

Figure 1. Reported PLK1 inhibitors.

trials, such as volasertib[34], rigosertib[35], and GSK461364[36] (Figure 1). In particular, the KD inhibitor volasertib (BI6727) has been granted orphan drug designation by the US FDA[37,38]. However, the lack of specificity that characterises many other KD inhibitors results in dose-limiting toxicities, severely restricting their development[33].

In our research, we discovered a novel, potent, and highly selective small molecule inhibitor targeting the KD domain of PLK1. First, the optimal pharmacophore models were constructed through the conformational relationship analysis of the KD domain structure of PLK1. Based on the key pharmacophore features, candidate molecules were screened from the compound database for conformational matches. Subsequently, the molecular docking screening of these compounds was performed based on the KD domain of PLK1, and five potential compounds (Hits 1–5) were identified. Hits 1–5 showed pM inhibitory potency against PLK1. Among them, Hit-4 was the most potent inhibitor of PLK1 and showed selective inhibition of PLK1. In addition, Hit-4 exhibited significant antiproliferative activity against DU-145 prostate cancer cells. In conclusion, our study has identified a small molecule inhibitor targeting PLK1 with high selectivity and inhibitory activity, which is worthy of further investigation.

Materials and methods

Cell culture and materials

The DU-145 prostate cancer cells used in this study were purchased from the American Type Culture Collection (ATCC), which is a reputable cell repository. ATCC follows strict guidelines and ethical protocols for the collection, authentication, and distribution of cell lines. We utilised these cells to perform *in vitro* antiproliferation assays to test the inhibitory effects of the tested compounds on cell proliferation. The cells were cultured in medium supplemented with 10% (v/v) foetal bovine serum, 50 units/ml of penicillin, and 50 µg/ml of streptomycin. The cell culture was maintained at 37 °C in a humid environment with 5% CO_2. Hit compounds were purchased from WuXi AppTec. Recombinant human PLK1 protein was purchased from Abcam (Cambridge, MA, USA).

Pharmacophore construction

The crystal structure of the PLK1 protein with its ligand (PDB ID: 3FC2) was retrieved from the Protein Data Bank (PDB) and was imported into the Molecular Operating Environment (MOE) for processing. First, the above structure was subjected to optimisation by the Quick Prep function in MOE, including the removal of unbound water molecules, the determination of partial charges, the attachment of polar hydrogen atoms, and energy minimisation processes. Then, the Ligand Interactions tool in MOE was utilised to analyse the interaction between PLK1 and the ligand to identify the key active binding sites. The Pharmacophore Query Editor tool in MOE was used to construct pharmacophore models based on the interaction analysis. In the Scheme menu, the EHT pharmacophore scheme was selected. Next, the key interaction point in the ligand was identified and the Feature tool was used to generate a series of pharmacophore features, including aromatic centres, hydrogen-bond acceptors, and hydrogen-bond donors.

Virtual screening

A chemical database of 35,000 compounds was constructed using combinatorial chemistry methods[39]. The two-dimensional (2D) structures of these compounds were then converted into three-dimensional (3D) conformations using the Conformation Import tool in MOE. The conformations were generated using the MMFF94x force field, and the Energy Minimisation module was used to ensure conformational stability. Then, the pharmacophore models constructed above for PLK1 were applied to perform a virtual screening of the compound database using the Pharmacophore Search panel. The Pharmacophore Search panel can be accessed directly from the Pharmacophore Query Editor. The conformation database was imported, and the Search module was used to initiate the search process. Next, the hits identified through pharmacophore screening were subjected to molecular docking into the KD of PLK1 for further evaluation. The Dock module within MOE was utilised to position each compound within the active site of PLK1. The docking results were evaluated using the Triangle Matcher method in association with the London

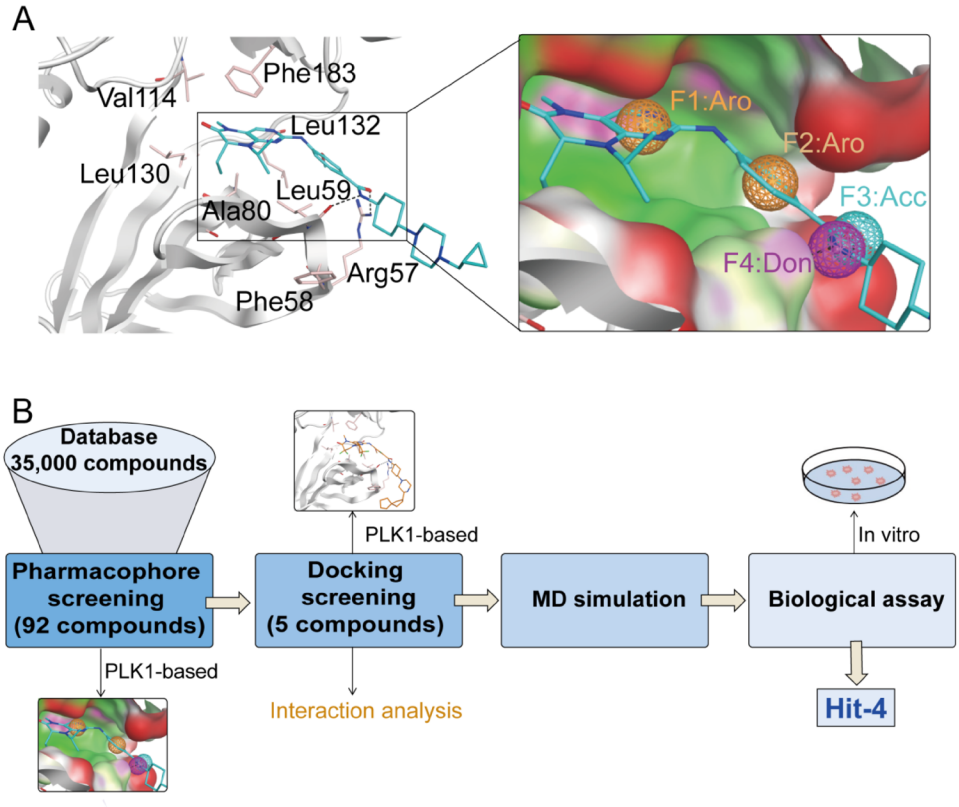

Figure 2. (a) The constructed pharmacophore models. (b) The workflow of combined virtual screening.

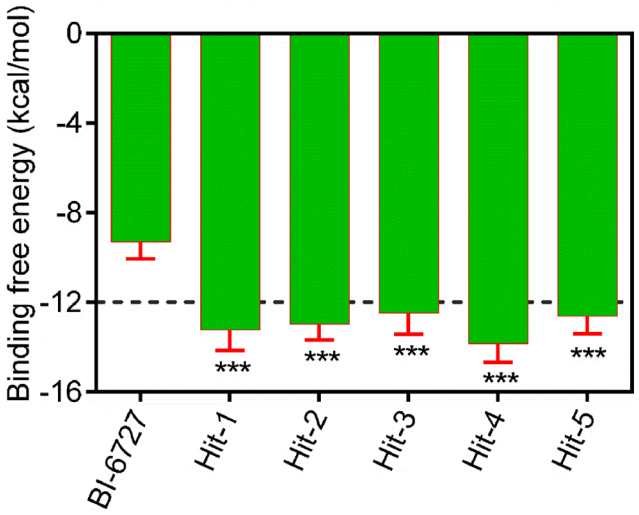

Figure 3. The binding free energy (kcal/mol) of five compounds (Hits 1–5). Data are expressed as mean ± SD, $n = 3$. ***$P < 0.001$ indicates a significant difference from the control group BI-6727.

dG scoring function. Comparing the binding free energies for different compound conformations, a lower docking score indicated a higher binding affinity.

PLK1 kinase inhibition assay

The assay was conducted as previously described[40]. The kinase reaction was performed in 384-well plates with a total assay volume of 5 µL per well, each well containing a reaction mixture consisting of 50 µM DTT, kinase and kinase substrate (25 ng PLK1 and 0.5 µg casein), 50 µM ATP and the tested compound at designated concentration (2.5, 5, 10, 20, 40, 80, 160, 320, 640, 1280, 2560 and 5120 pM). The tested compound solution (1 µL) was replaced with 5% DMSO for positive control wells, while negative control wells contained neither the tested compound nor enzyme. Each well was incubated for 60 min at room temperature. Subsequently, 5 µL of ADP-Glo reagent was added to each well and incubated for 40 min to terminate the reaction. ADP was then converted to ATP by adding 10 µL of kinase detection reagent and incubating for 30 min. Then, the luminescence of ATP was measured using the Victor Nivo Multimode Microplate Reader, and the following formula was used to calculate kinase activity: kinase activity% = [(luminescence of compound - luminescence of negative control)/(luminescence of positive control - luminescence of negative control)] × 100%. IC_{50} values were determined by analysing dose-response curves using Graph Prism 8.0 software.

Selectivity assays

The selectivity profile of Hit-4 was determined by evaluating its inhibitory activity against a panel of 69 kinases containing other polo-like kinases. The experiment was conducted by ICE Bioscience Inc. (Beijing, China). The LanthaScreen™ Eu Kinase Binding Assay was performed to evaluate the selectivity profile of Hit-4 on a panel of 69 kinases.

Molecular dynamics simulation

The crystal structures of PLK1 (PDB ID: 3FC2) was obtained from the PDB. MD simulations were performed using GROMACS

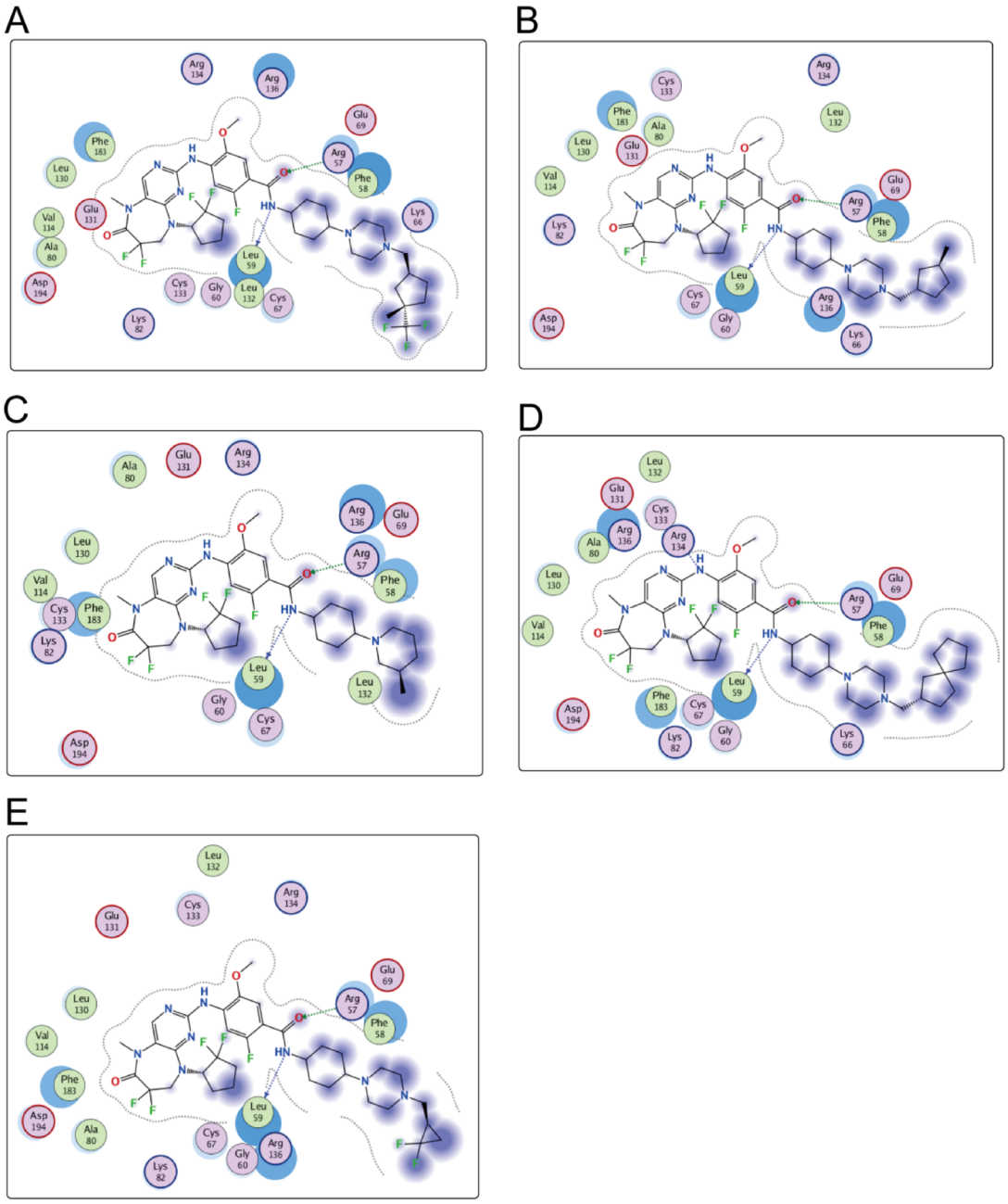

Figure 4. (a-e) The 2D interactions of Hits 1–5 with PLK1, respectively. Green spheres represent hydrophobic amino acids in PLK1, purple spheres represent polar amino acids in PLK1, green and blue dashed arrows represent hydrogen bonds.

(version 2022). The topology of PLK1 was generated under the AMBER99SB-ILDN force field. Hit-1 and Hit-4 were processed through the Acpype Server (www.bio2byte.be) to generate their respective topology files. Subsequently, the topology files for the ligands were merged with the protein topology file to create the complete complex system, respective. The system was solvated using the SPC/E water model within a cubic box of 1.0 nm. The sodium (Na^+) and chloride (Cl^-) ions were added to maintain charge neutrality. Next, the steepest descent algorithm with 5000 steps was used to minimise the system energy. The system temperature was maintained at 300 K during a 100 ps NVT simulation. A 100 ps NPT simulation was then performed to keep the pressure at 1 bar. Finally, a 50 ns MD simulation was performed on the system. The 50 ns MD simulation has been used in several previous protein-ligand interaction stability studies by our research group and it was found that energy equilibrium was reached and the simulation results were highly reliable at 50 ns MD simulation duration[41,42]. These data were processed using Prism 8.0 software.

In vitro *antiproliferation assay*

A density of 5×10^4 cells per well was inoculated into 96-well plates and incubated overnight. Varying concentrations of Hits 1–5 were introduced into each well, and the plates were incubated at 37 °C for 72 h. Following incubation, the culture medium was aspirated and MTT solution (with a concentration of 5 mg/mL) was dispensed into each well for a further incubation period of 4 h. The supernatant was then removed via centrifugation, followed by the addition of DMSO to solubilise the precipitated crystals. Ultimately, absorbance was

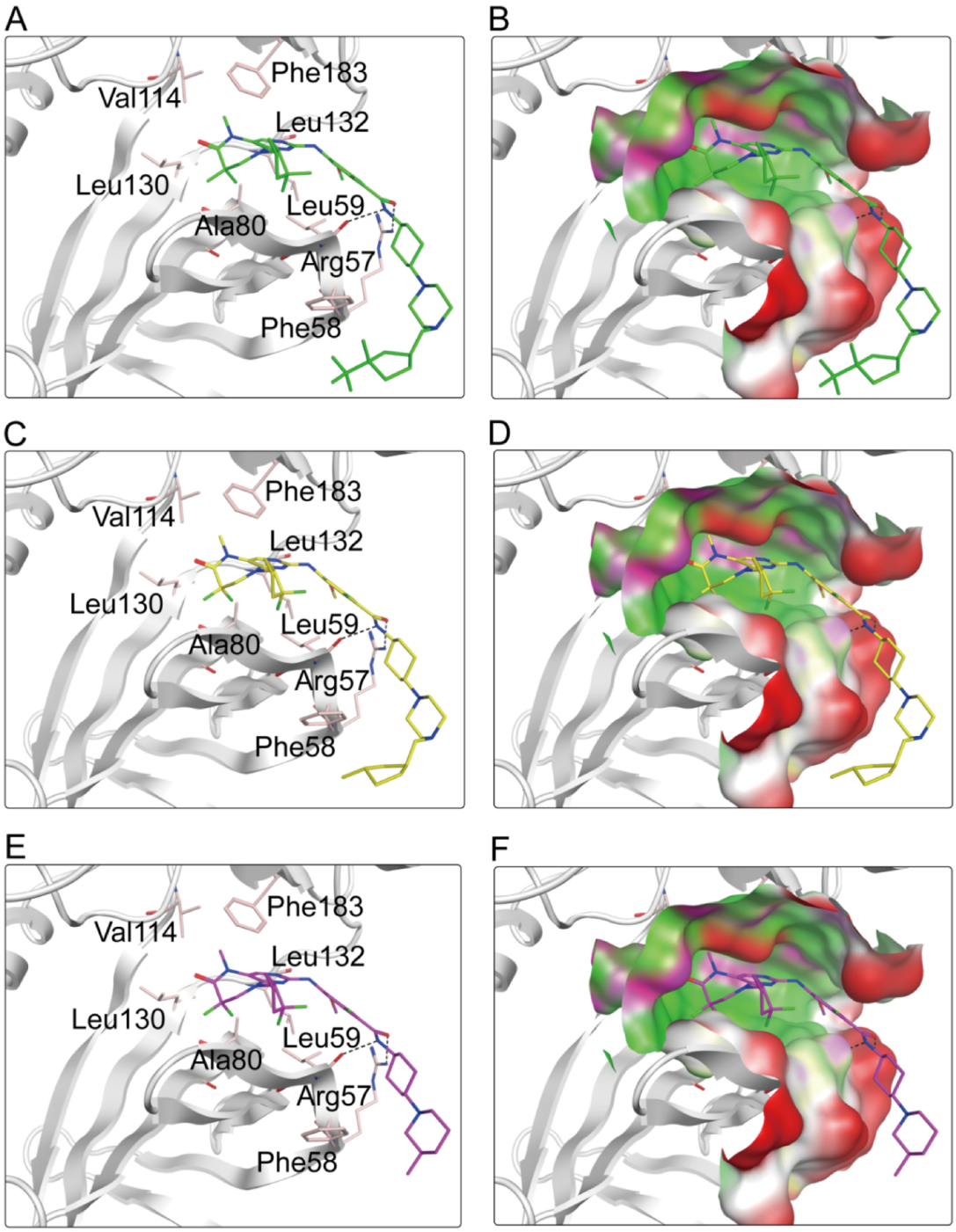

Figure 5.The binding modes of Hits 1–5 within the PLK1 binding pocket are shown as follows: (a, b) Hit-1 is shown in green; (c, d) Hit-2 is shown in yellow; (e, f) Hit-3 is shown in purple; (g, h) Hit-4 is shown in orange; (i, j) Hit-5 is shown in blue. Active site residues are shown as pink sticks. Hydrogen bonds are represented in black dashed lines.

measured at 570 nm using a microplate reader. The non-linear regression was used to plot a dose-response curve and determine the IC_{50} value. Data analysis was performed using Prism 8.0 software.

Results and discussion

Pharmacophore construction

The pharmacophore models were constructed based on a detailed analysis of the binding site interaction between PLK1 and its ligand BI6727 (PDB ID: 3FC2). First, the Ligand Interaction module within MOE was employed to assess the structure-activity relationship between PLK1 and BI6727, and identified key interaction elements for pharmacophore models construction (Figure 2a). The ligand made hydrophobic contacts with the residues Phe58, Ala80, Val114, Leu130, Leu132, and Phe183 of PLK1, prompting the inclusion of aromatic features in the pharmacophore model. In addition, the amide CO group of the ligand formed a hydrogen bond with Arg57 of PLK1, providing a hydrogen-bond acceptor feature, while NH group of the ligand created a hydrogen bond with the

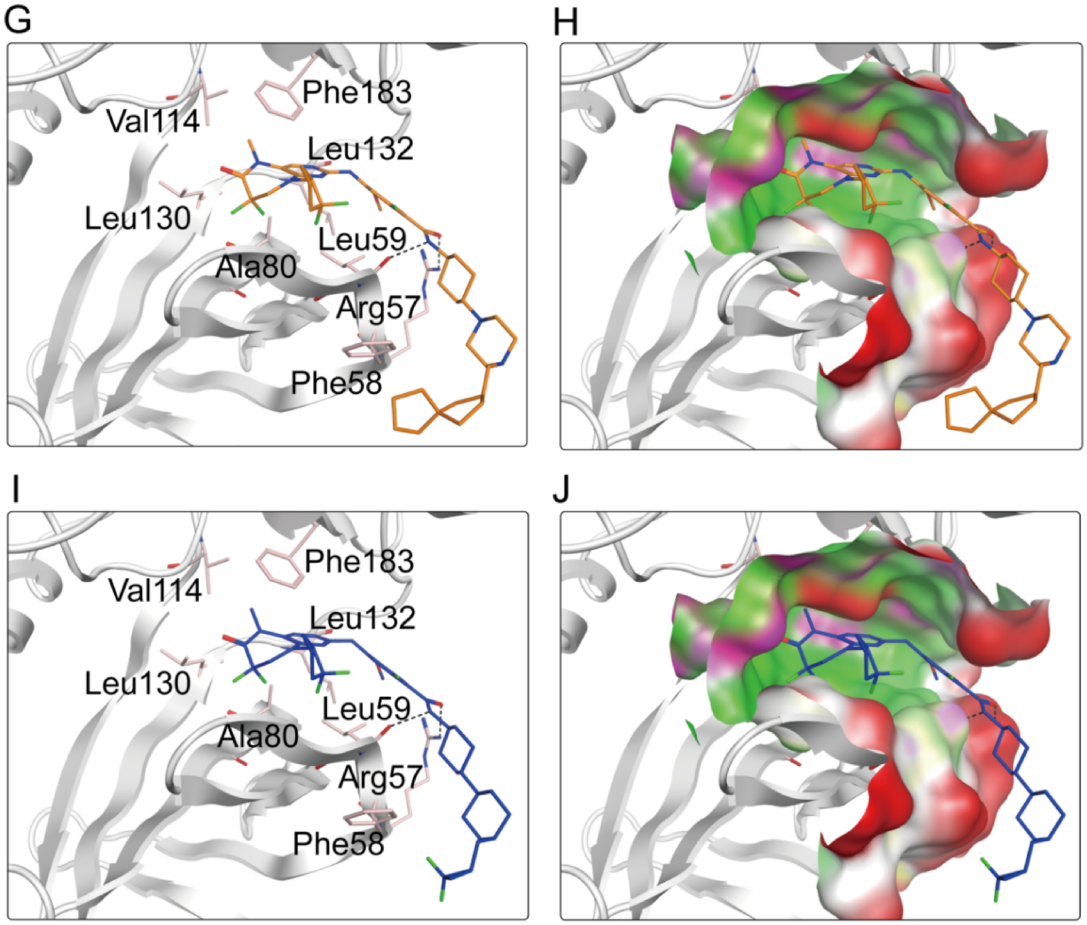

Figure 5. Continued.

Table 1. PLK1 residues forming key binding interactions with Hits 1–5.

	Hydrogen bonding interactions			
Name	Amino acid involved	Hydrogen bonds	Bond distance (Å)	Hydrophobic interactions
Hit-1	Arg57	O•••H-N	2.83	Phe58, Ala80, Val114, Leu130,
	Leu59	H-N•••O	2.97	Leu132, Phe183
Hit-2	Arg57	O•••H-N	2.83	Phe58, Ala80, Val114, Leu130,
	Leu59	H-N•••O	3.00	Leu132, Phe183
Hit-3	Arg57	O•••H-N	2.85	Phe58, Ala80, Val114, Leu130,
	Leu59	H-N•••O	2.97	Leu132, Phe183
Hit-4	Arg57	O•••H-N	2.84	Phe58, Ala80, Val114, Leu130,
	Leu59	H-N•••O	3.00	Leu132, Phe183
Hit-5	Arg57	O•••H-N	2.83	Phe58, Ala80, Val114, Leu130,
	Leu59	H-N•••O	2.97	Leu132, Phe183

Table 2. The inhibitory effects of Hits 1–5 on PLK1 and DU-145 cells.

Name	PLK1 (IC_{50}, pM)[a]	DU-145 (IC_{50}, nM)[b]
Hit-1	39.46 ± 2.79	0.18 ± 0.02
Hit-2	47.35 ± 3.21	0.23 ± 0.04
Hit-3	68.32 ± 5.28	0.35 ± 0.05
Hit-4	22.61 ± 1.12	0.09 ± 0.01
Hit-5	56.82 ± 3.34	0.47 ± 0.06
BI-6727	871.04 ± 16.15	4.03 ± 0.15

[a]IC_{50} (pM) is the concentration of compound needed to achieve 50% inhibition of enzyme activity treated with Hits 1–5.
[b]IC_{50} (nM) is the concentration of compound needed to reduce cell growth by 50% after 72 h treatment with Hits 1–5.
The data are presented as the mean ± SD, $n = 3$.

key residue Leu59 of PLK1, establishing a hydrogen-bond donor feature. Consequently, four critical pharmacophore features were constructed: two aromatic features (F1 and F2: Aro), one hydrogen-bond acceptor feature (F3: Acc), and one hydrogen-bond donor feature (F4: Don). These pharmacophore models with essential chemical features are pivotal for the identification of potential PLK1 inhibitors.

Virtual screening

In this study, a combined virtual screening approach including pharmacophore screening, molecular docking, MD simulation, and biological assays was employed to discover novel PLK1 inhibitors. The virtual screening workflow is illustrated in Figure 2b. First, the 2D database consisting of 35,000 compounds was converted into 3D structure. The above four pharmacophore features (F1 and F2: Aro, F3: Acc, F4: Don) were then applied to filter the database, and a total of 92 compounds were identified that matched the Aro, Acc, and Don features. Subsequently, these 92 compounds were docked into the KD domain of PLK1, with docking scores indicating binding affinity—lower scores corresponding to stronger affinities. The top five compounds with the lowest docking scores were selected as optimal hits. As shown in Figure 3, five top hits (Hits 1–5) with the lowest scores were selected from 92 compounds. Notably, the docking scores of Hits 1–5 were lower than the known PLK1 inhibitor BI-6727 (docking score of −9.31 kcal/mol), suggesting superior binding affinities. Among these, Hit-4 demonstrated the lowest docking score, indicative of the strongest bind-

Table 3. Kinase selectivity profile of Hit-4 at a concentration of 10 μM on a panel of 69 kinases.

Target	% Inhibition at 10 μM	Target	% Inhibition at 10 μM	Target	% Inhibition at 10 μM
ABL1	0.70 ± 0.01	FES	4.79 ± 0.12	LTK	3.51 ± 0.09
ABL2	0.08 ± 0.02	FGFR1	0.87 ± 0.03	LYN	0.62 ± 0.04
AXL	0.40 ± 0.05	FGFR2	0.75 ± 0.04	MERTK	0.19 ± 0.01
BLK	0.69 ± 0.03	FGFR3	5.51 ± 0.16	MET	8.12 ± 0.17
BMX	2.03 ± 0.06	FGFR4	2.84 ± 0.07	MST1R	7.45 ± 0.11
BTK	3.10 ± 0.08	FGR	0.45 ± 0.03	MUSK	0.94 ± 0.05
CSF1R	1.22 ± 0.05	FRK	6.49 ± 0.22	NTRK1	0.75 ± 0.06
EGFR	0.49 ± 0.04	FYN	0.08 ± 0.01	NTRK2	1.81 ± 0.09
DDR1	0.19 ± 0.01	PIM1	0.32 ± 0.03	NTRK3	5.03 ± 0.17
DDR2	3.48 ± 0.09	RAF1	6.19 ± 0.24	PDGFRA	0.61 ± 0.04
ALK	0.91 ± 0.03	ROS1	0.66 ± 0.05	PDGFRB	5.71 ± 0.12
EPHA1	0.96 ± 0.05	ZAK	0.33 ± 0.02	PTK2	3.08 ± 0.06
EPHA2	0.61 ± 0.04	TYRO3	0.90 ± 0.04	CDK5	0.68 ± 0.04
EPHA3	0.79 ± 0.07	YES1	0.20 ± 0.01	CDK6	4.18 ± 0.08
EPHA4	0.45 ± 0.03	ZAP70	6.09 ± 0.17	CDK7	7.58 ± 0.13
EPHA5	2.86 ± 0.08	HCK	1.44 ± 0.08	CDK8	5.28 ± 0.09
EPHA6	4.17 ± 0.07	IGF1R	0.49 ± 0.03	KIT	0.77 ± 0.04
EPHA7	0.30 ± 0.01	INSR	0.15 ± 0.01	KDR	0.14 ± 0.01
EPHA8	0.73 ± 0.04	INSRR	0.34 ± 0.04	ERBB2	6.41 ± 0.15
EPHB1	0.93 ± 0.03	ITK	0.70 ± 0.05	PLK2	0.73 ± 0.03
EPHB2	0.68 ± 0.06	JAK1	0.90 ± 0.03	PLK3	0.24 ± 0.01
EPHB3	0.53 ± 0.02	JAK2	7.69 ± 0.27	PLK4	1.87 ± 0.07
EPHB4	2.77 ± 0.08	JAK3	6.51 ± 0.18	PLK5	0.48 ± 0.02

The data are presented as the mean ± SD, $n = 3$.

ing to PLK1. The structures of Hits 1–5 are presented in Figure 4. Next, the molecular interactions of these five compounds with PLK1 were analysed in detail to validate the screening findings.

Interaction analysis

The molecular interactions of the five hits (Hits 1–5) with PLK1 were analysed and the possible binding modes are shown in Figures 4 and 5. The hydrogen bonding and hydrophobic interactions between Hits 1–5 and PLK1 are shown in Table 1. The ligands formed hydrophobic interactions with the key residues Phe58, Ala80, Val114, Leu130, Leu132, and Phe183, consistent with the Aro (F1 and F2) pharmacophore features. In particular, the 1-methyl-1-(trifluoromethyl)cyclopentane group at the terminal end of Hit-1 and the spiro-nonane group at the terminal end of Hit-4 are relatively hydrophobic. Meanwhile, the amide group in the ligand formed hydrogen bond interactions with the residues Leu59 and Arg57 of PLK1, corresponding to the Acc (F3) and Don (F4) pharmacophore features, respectively. Moreover, the surface maps showed that the PLK1 active pocket was well matched in shape to Hits 1–5. Notably, the 1-methyl-1-(trifluoromethyl)cyclopentane group at the end of Hit-1 and the spiro-nonane group at the end of Hit-4 showed excellent shape complementarity with the active pocket of PLK1. In conclusion, Hits 1–5 showed significant interactions with key residues within the active sites of PLK1 and perfectly matched to the binding pocket of PLK1, especially Hit-1 and Hit-4. Based on the favourable binding pattern analysis, the inhibitory potential of Hits 1–5 was evaluated.

In vitro PLK1 inhibitory activity

Enzyme inhibition assay was performed to evaluate inhibitory potency of Hits 1–5 on PLK1. As shown in Table 2, Hits 1–5 exhibited significant inhibitory activity against PLK1 with IC_{50} values ranging from approximately 22.61 to 68.32 pM, which were superior to those of the positive control BI-6727. Notably, Hit-4 had the strongest inhibitory activity against PLK1 (IC_{50} = 22.61 ± 1.12 pM) with an approximately 38-fold lower IC_{50} value compared to BI-6727. In addition, we performed a comparison of the IC_{50} values between the reported PLK1 KD inhibitors (0.83-4 nM) and Hits 1–5 (22.61-68.32 pM). The results indicate that Hits 1–5 exhibited significantly stronger inhibitory activity than the reported PLK1 KD inhibitors (Table S1).

In addition, selectivity assays were conducted on a panel of 69 kinases to further evaluate the selective inhibitory effect of Hit-4. As shown in Table 3, Hit-4 exhibited an inhibition rate of less than 10% against these kinases at a concentration of 10 μM. These results suggest that Hit-4 selectively targets PLK1 for inhibition.

MD simulation

Since Hit-1 and Hit-4 were perfectly matched to the active pocket of PLK1 and both showed strong inhibitory activity against PLK1, MD simulations were performed using GROMACS to assess their binding stability to PLK1. The smaller variation of the root mean square deviation (RMSD) value indicates the better binding stability of the complex. Figure 6a and 6b showed that the RMSD of both PLK-Hit-1 and PLK-Hit-4 complexes reached a stable value with slight fluctuations around 0.2 nm. This indicates that the binding of Hit-1 and Hit-4 to PLK1 is stable. The root mean square fluctuation (RMSF) provides insight into the flexibility of amino acids involved in ligand binding. In Figure 6c and 6d, the RMSF values of the key residues Arg57, Phe58, Leu59, Ala80, Val114, Leu130, Leu132, and Phe183 in the binding site of PLK1 were less than 0.13 nm, reflecting the stable binding of the key amino acids of PLK1 to Hit-1 and Hit-4. In addition, Figure 6e and 6f) showed that the radius of gyration (Rg) value of PLK1 was stable at around 2.05 nm, indicating that the protein maintained structural integrity during the simulation. In Figure 6g and 6h, no significant changes in the secondary structure of the PLK1 were observed, indicating that the protein remained structurally stable after complexation with Hit-1 and Hit-4. In summary, Hit-1 and Hit-4 are able to bind stably to the active site of PLK1 and maintain the structural stability of the complex throughout the simulation.

Inhibition of cell growth

MTT assays were conducted to assess the inhibitory effects of Hits 1–5 on the proliferation of DU-145 prostate cancer cells. As shown in Table 2, Hits 1–5 and the positive control BI-6727 exhibited different degrees of antiproliferative activity against DU-145 cells, and the inhibitory activity of Hits 1–5 was significantly higher than that of BI-6727. Among them, Hit-4 was the most potent compound in inhibiting the growth of DU-145 cells (IC_{50} = 0.09 ± 0.01 nM). These data suggest that Hit-4 has potential therapeutic efficacy, making it a promising candidate for prostate cancer treatment.

Conclusions

PLK1 is overexpressed in prostate cancer and is one of the top five signalling pathways upregulated in castration-resistant prostate cancer, highlighting the importance of developing potent PLK1 inhibitors as a therapeutic strategy for prostate cancer. In this study, we successfully identified five novel and potent PLK1 inhibitors (Hits 1–5) using a combined virtual screening protocol. Based on the constructed pharmacophore features of PLK1, we screened the candidate molecules from a compound database. These

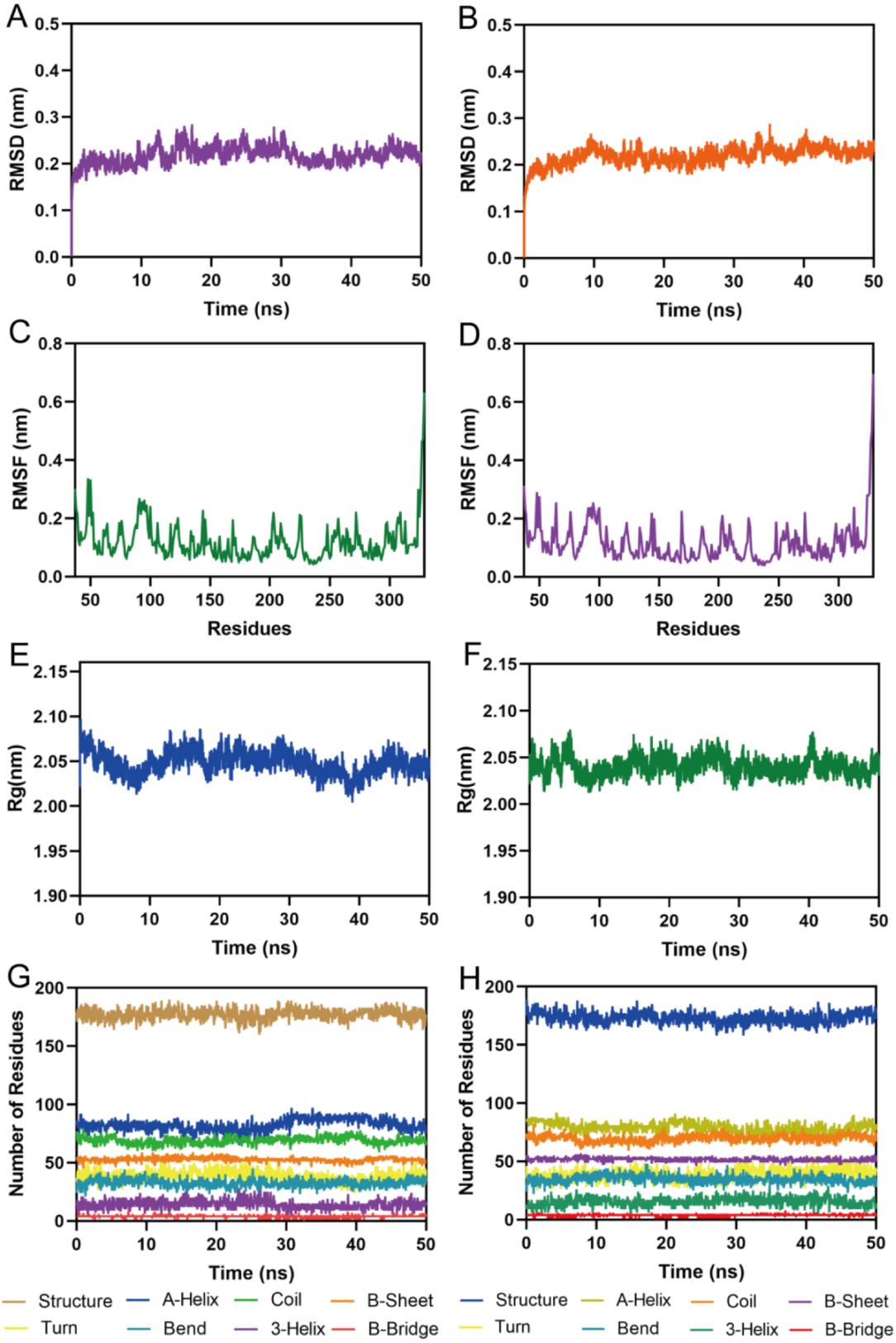

Figure 6. MD simulation of PLK1 in complex with Hit-1 and Hit-4. (a) RMSD of Hit-1 in PLK1-Hit-1 complex. (b) RMSD of Hit-4 in PLK1-Hit-4 complex. (c, d) RMSF of PLK1 residues in the complex of PLK1-Hit-1 and PLK1-Hit-4, respectively. (e, f) Rg of PLK1 in the complex of PLK1-Hit-1 and PLK1-Hit-4, respectively. (g, h) The secondary structures of PLK1 in the complex of PLK1-Hit-1 and PLK1-Hit-4, respectively.

compounds were then docked into the KD domain of PLK1 and five potential compounds (Hits 1–5) were identified. The structures of Hits 1–5 showed compatibility with the active site pocket of PLK1, especially Hit-4. Enzyme inhibition assay showed that Hits 1–5 exhibited pM inhibitory potency against PLK1, and Hit-4 had the strongest inhibitory activity. Notably, Hit-4 selectively targeted

PLK1 for inhibition without significant inhibitory effects on other kinases. The concordance between inhibitory activity and docking scores demonstrated the effectiveness of the combined virtual screening approach in predicting the activity of lead compounds. Importantly, Hit-4 displayed significant antiproliferative activity against DU-145 prostate cancer cells.

Given the excellent *in vitro* antiproliferative activity of Hit-4 against DU-145 cells, we believe that Hit-4 is a promising new anti-prostate cancer candidate worthy of further *in vivo* evaluation in mice to assess its therapeutic potential and safety profile. In addition, the development of Hit-4 may face some challenges, including the potential emergence of drug resistance and the need for combination therapies to improve therapeutic efficacy. Combinations of some PLK1 inhibitors with chemotherapy and targeted therapies have shown promising results in numerous cancer treatment studies both *in vitro* and *in vivo*[43]. This suggests that the combination of Hit-4 with other therapeutic agents may offer superior efficacy compared to monotherapy, making it an attractive strategy to enhance treatment outcomes. Therefore, advancing Hit-4 into *in vivo* studies in mice is essential to evaluate its safety profile and address potential challenges in drug development. In conclusion, we have identified Hit-4 as a highly selective PLK1 inhibitor with pM inhibitory activity, demonstrating significant potential for the treatment of prostate cancer and warranting further investigation.

Author contributions

ZX, LG, and YW performed experiments and acquired data. ZX, LG, and MMN collected experimental samples. ZX, MMN, and YR performed statistical analysis. CX and LY analysed data and wrote the paper. All authors had edited and approved the final manuscript.

Ethical statement

The cell culture and experimental procedures were conducted in accordance with standard laboratory practices and guidelines. We did not perform any procedures that would require additional specific ethical approvals beyond the standard practices for cell culture and experimentation in a laboratory setting, as this study used commercially available cell lines and the experiments did not involve any procedures that could potentially harm humans or animals.

Disclosure statement

The authors declare that the research was conducted in the absence of any commercial or financial relationships that could be construed as a potential conflict of interest.

Funding

This research was supported by the Taizhou People's Hospital (Taizhou, Jiangsu, China; Grant No. ZL202220).

Data availability statement

The original contributions presented in the study are included in the article, further inquiries can be directed to the corresponding author/s.

References

1. Sung H, Ferlay J, Siegel RL, Laversanne M, Soerjomataram I, Jemal A, Bray F. Global cancer statistics 2020: GLOBOCAN estimates of incidence and mortality worldwide for 36 cancers in 185 countries. CA Cancer J Clin. 2021;71(3):209–249.
2. Sekhoacha M, Riet K, Motloung P, Gumenku L, Adegoke A, Mashele S. Prostate cancer review: genetics, diagnosis, treatment options, and alternative approaches. Molecules. 2022; 27(17):5730.
3. Ong S, O'Brien J, Medhurst E, Lawrentschuk N, Murphy D, Azad A. Current treatment options for newly diagnosed metastatic hormone-sensitive prostate cancer-a narrative review. Transl Androl Urol. 2021;10(10):3918–3930.
4. Yamada Y, Beltran H. The treatment landscape of metastatic prostate cancer. Cancer Lett. 2021;519:20–29.
5. Peng J, Nouri M, Maasoumyhaghighi H, Liu J, Liu X. Plk1, a promising THERAPEUTIC target for prostate cancer treatment. Serican J Med. 2024;1(1):23189.
6. Figueiredo A, Costa L, Maurício MJ, Figueira L, Ramos R, Martins-da-Silva C. Nonmetastatic castration-resistant prostate cancer: current challenges and trends. Clin Drug Investig. 2022;42(8):631–642.
7. Swami U, McFarland TR, Nussenzveig R, Agarwal N. Advanced prostate cancer: treatment advances and future directions. Trends Cancer. 2020;6(8):702–715.
8. Chapagai D, Merhej G, McInnes C, Wyatt MD. Structural basis for variations in polo-like kinase 1 conformation and intracellular stability induced by ATP-competitive and novel noncompetitive abbapolin inhibitors. ACS Chem Biol. 2023;18(7):1642–1652.
9. Chiappa M, Petrella S, Damia G, Broggini M, Guffanti F, Ricci F. Present and future perspective on PLK1 inhibition in cancer treatment. Front Oncol. 2022;12:903016.
10. Shakeel I, Basheer N, Hasan GM, Afzal M, Hassan MI. Polo-like Kinase 1 as an emerging drug target: structure, function and therapeutic implications. J Drug Target. 2021;29(2):168–184.
11. Kalous J, Aleshkina D. Multiple roles of PLK1 in mitosis and meiosis. Cells. 2023;12(1):187.
12. Gheghiani L, Wang L, Zhang Y, Moore XTR, Zhang J, Smith SC, Tian Y, Wang L, Turner K, Jackson-Cook CK, et al. PLK1 induces chromosomal instability and overrides cell-cycle checkpoints to drive tumorigenesis. Cancer Res. 2021;81(5):1293–1307.
13. Alverez CN, Park J-E, Toti KS, Xia Y, Krausz KW, Rai G, Bang JK, Gonzalez FJ, Jacobson KA, Lee KS. Identification of a new heterocyclic scaffold for inhibitors of the polo-box domain of polo-like kinase 1. J Med Chem. 2020;63(22):14087–14117.
14. Iliaki S, Beyaert R, Afonina IS. Polo-like kinase 1 (PLK1) signaling in cancer and beyond. Biochem Pharmacol. 2021;193: 114747.
15. Lashen AG, Toss MS, Wootton L, Green AR, Mongan NP, Madhusudan S, Rakha E. Characteristics and prognostic significance of polo-like kinase-1 (PLK1) expression in breast cancer. Histopathology. 2023;83(3):414–425.
16. Liu B, Meng L-B, Su J-Z, Fan B, Zhao S-B, Wang H-Y, Li T, Wang T-Y, Zhang A-L, Ni X-C. Plk1 as one novel target for the poor prognosis of bladder cancer: an observational study. Medicine (Baltimore). 2022;101(39):e30723.
17. Wu J, Ivanov AI, Fisher PB, Fu Z. Polo-like kinase 1 induces epithelial-to-mesenchymal transition and promotes epithelial cell motility by activating CRAF/ERK signaling. Elife. 2016;5:e10734.
18. Kachouh E. PLK1 overexpression drives tumorigenesis in a prostate cancer mouse model [master's thesis]. [Richmond (VA)]: Virginia Commonwealth University; 2024.

19. Javed A, Özduman G, Altun S, Duran D, Yerli D, Özar T, Şimşek F, Korkmaz KS. Mitotic kinase inhibitors as therapeutic interventions for prostate cancer: evidence from in vitro studies. Endocr Metab Immune Disord Drug Targets. 2023;23(14):1699–1712.
20. Li J, Wang R, Kong Y, Broman MM, Carlock C, Chen L, Li Z, Farah E, Ratliff TL, Liu X. Targeting Plk1 to enhance efficacy of olaparib in castration-resistant prostate cancer. Mol Cancer Ther. 2017;16(3):469–479.
21. Peng Y, Liu Y, Gao Y, Yuan B, Qi X, Fu Y, Zhu Q, Cao T, Zhang S, Yin L, et al. USP7 is a novel Deubiquitinase sustaining PLK1 protein stability and regulating chromosome alignment in mitosis. J Exp Clin Cancer Res. 2019;38(1):1–12.
22. Zhu Z, West GR, Wang DC, Collins AB, Xiao H, Bai Q, Mesfin FB, Wakefield MR, Fang Y. AFP peptide (AFPep) as a potential growth factor for prostate cancer. Med Oncol. 2021;39(1):2.
23. Gogacz M, Peszke J, Natorska-Chomicka D, Makuch-Kocka A, Szewczyk KD. Anticancer effects of propolis extracts obtained with the cold separation method on PC-3 and DU-145 prostate cancer cell lines. Molecules. 2022;27(23):8245.
24. Wu JG, Ivanov AI, Fisher PB, Fu Z. Polo-like kinase 1 induces epithelial-to-mesenchymal transition and promotes epithelial cell motility by activating CRAF/ERK signaling. Elife. 2016;5: e10734.
25. Wissing MD, Mendonca J, Kortenhorst MSQ, Kaelber NS, Gonzalez M, Kim E, Hammers H, van Diest PJ, Carducci MA, Kachhap SK. Targeting prostate cancer cell lines with polo-like kinase 1 innibitors as a single agent and in combination with histone deacetylase inhibitors. FASEB J. 2013;27(10):4279–4293.
26. Li W, Hao Y. Polo-like kinase 1 and DNA damage response. DNA Cell Biol. 2024;43(9):430–437.
27. Stafford JM, Wyatt MD, McInnes C. Inhibitors of the PLK1 polo-box domain: drug design strategies and therapeutic opportunities in cancer. Expert Opin Drug Discov. 2023;18(1):65–81.
28. La YK, Gunasekaran P, Yim MS, Lee G-H, Hwang YS, Damodharan K, Kim M-H, Bang JK, Ryu EK. Synthesis and evaluation of small molecule-based derivatives as inhibitors of polo-box domain of polo-like kinase-1. J Anal Sci Technol. 2023;14(1):48.
29. Moore XT, Gheghiani L, Fu Z. The role of polo-like kinase 1 in regulating the forkhead box family transcription factors. Cells. 2023;12(9):1344.
30. Lee KS, Burke TR, Park J-E, Bang JK, Lee E. Recent advances and new strategies in targeting Plk1 for anticancer therapy. Trends Pharmacol Sci. 2015;36(12):858–877.
31. Normandin K, Lavallée J-F, Futter M, Beautrait A, Duchaine J, Guiral S, Marinier A, Archambault V. Identification of Polo-like kinase 1 interaction inhibitors using a novel cell-based assay. Sci Rep. 2016;5(1):37581.
32. Gutteridge REA, Ndiaye MA, Liu X, Ahmad N. Plk1 inhibitors in cancer therapy: from laboratory to clinics. Mol Cancer Ther. 2016;15(7):1427–1435.
33. Zhang J, Zhang L, Wang J, Ouyang L, Wang Y. Polo-like kinase 1 inhibitors in human cancer therapy: development and therapeutic potential. J Med Chem. 2022;65(15):10133–10160.
34. Schöffski P, Awada A, Dumez H, Gil T, Bartholomeus S, Wolter P, Taton M, Fritsch H, Glomb P, Munzert G. A phase I, dose-escalation study of the novel Polo-like kinase inhibitor volasertib (BI 6727) in patients with advanced solid tumours. Eur J Cancer. 2012;48(2):179–186.
35. Bowles DW, Diamond JR, Lam ET, Weekes CD, Astling DP, Anderson RT, Leong S, Gore L, Varella-Garcia M, Vogler BW, et al. Phase I study of oral rigosertib (ON 01910.Na), a dual inhibitor of the PI3K and Plk1 pathways, in adult patients with advanced solid malignancies. Clin Cancer Res. 2014;20(6): 1656–1665.
36. Olmos D, Barker D, Sharma R, Brunetto AT, Yap TA, Taegtmeyer AB, Barriuso J, Medani H, Degenhardt YY, Allred AJ, et al. Phase I study of GSK461364, a specific and competitive polo-like kinase 1 inhibitor, in patients with advanced solid malignancies. Clin Cancer Res. 2011;17(10):3420–3430.
37. Bose P, Grant S. Orphan drug designation for pracinostat, volasertib and alvocidib in AML. Leuk Res. 2014;38(8):862–865.
38. Wei X, Song M, Huang C, Yu Q, Jiang G, Jin G, Jia X, Shi Z. Effectiveness, safety and pharmacokinetics of Polo-like kinase 1 inhibitors in tumor therapy: a systematic review and meta-analysis. Front Oncol. 2023;13:1062885.
39. Zhou YJ, Tang S, Chen TT, Niu MM. Structure-based pharmacophore modeling, virtual screening, molecular docking and biological evaluation for identification of potential poly (ADP-ribose) polymerase-1 (PARP-1) inhibitors. Molecules. 2019;24(23):4258.
40. Cheng ZX, Hwang SS, Bhave M, Rahman T, Wezen XC. Combination of QSAR modeling and hybrid-based consensus scoring to identify dual-targeting inhibitors of PLK1 and p38γ. J Chem Inf Model. 2023;63(21):6912–6924.
41. Zheng LF, Zhang YX, Mei S, Xie TY, Zou YT, Wang YT, Jing H, Xu ST, Dramou P, Xu Z, et al. Discovery of a potent dual son of sevenless 1 (SOS1) and epidermal growth factor receptor (EGFR) inhibitor for the treatment of prostate cancer. J Med Chem. 2024;67(9):7130–7145.
42. Zhang L, Guan LX, Wang YT, Niu MM, Yan JH. Discovery of a dual-target DYRK2 and HDAC8 inhibitor for the treatment of hepatocellular carcinoma. Biomed Pharmacother. 2024;177:116839.
43. Su S, Chhabra G, Singh CK, Ndiaye MA, Ahmad N. PLK1 inhibition-based combination therapies for cancer management. Transl Oncol. 2022;16:101332.